Int J Biometeorol (2003) 47:126–138
DOI 10.1007/s00484-003-0164-4

ORIGINAL ARTICLE

Rikie Suzuki · Tomoyuki Nomaki · Tetsuzo Yasunari

West–east contrast of phenology and climate in northern Asia revealed using a remotely sensed vegetation index

Received: 14 May 2002 / Revised: 6 January 2003 / Accepted: 6 January 2003 / Published online: 2 April 2003

Abstract The phenology of the vegetation covering north Asia (mainly Siberia) and its spatial characterstics were investigated using remotely sensed normalized difference vegetation index (NDVI) data. The analysis used the weekly averaged NDVI over 5 years (1987–1991) using the second-generation weekly global vegetation index dataset (0.144°× 0.144° spatial resolution). In the seasonal NDVI cycle, three phenological events were defined for each pixel: green-up week (NDVI exceeds 0.2), maximum week, and senescence week (NDVI drops below 0.2). Generally there was a west-early/east-late gradient in the three events in north Asia. In the zonal transect between 45° and 50°N, the timing of green-up, maximum, and senescence near 60°E (Kazakh) was about 3.4, 8.7, and 13.4 weeks earlier than near 110°E (Mongolia) respectively. It has been suggested that vegetation near Kazakh only flourishes during a short period when water from snow melt is available from late spring to early summer. In Mongolia, abundant water is available for the vegetation, even in midsummer, because of precipitation. In the 50–60°N zonal transect, the green-up and maximum near 40°E were about 3.8 and 3.9 weeks earlier than near 115°E, respectively. As for the week of senescence, there was no clear west–east trend. This west-to-east phenological gradient was related to the weekly cumulative temperature (over 0 °C). Weeks in which the cumulative temperature exceeded 40 °C and 140 °C had a similar west-east distribution to green-up and maximum NDVI.

Keywords Taiga · Siberia · Phenology · Green-wave · NDVI · Soil moisture

R. Suzuki (✉)
IGCR, Frontier Research System for Global Change,
3173-25 Showamachi, Kanazawa-ku, Yokohama,
Kanagawa 236-0001, Japan,
e-mail: rikie@jamstec.go.jp
Tel.: +81-45-778-5541
Fax: +81-45-778-5706

T. Nomaki
Data Analysis and Research Division,
Remote Sensing Technology Center of Japan (RESTEC),
Tokyo, Japan

T. Yasunari
Hydrospheric Atmospheric Research Center (HyARC),
Nagoya University, Nagoya, Japan IGCR,
Frontier Research System for Global Change, Yokohama, Japan

Introduction

Vegetation cover is strongly characterized by the climate of a region, as noted in many reports (Walter 1973; Woodward 1987). For example, larch forests in Siberian taiga are dormant during the winter, and then green with foliation as temperatures warm in spring and summer, reaching the mature stage in summer. In autumn, senescence follows a drop in temperature. This phenology–climate relationship is an important theme that has been broadly investigated from the perspective of plant geography.

Since the 1980s, global vegetation data have been available from satellite measurements. Currently, massive amounts of information on vegetation are available for climatological and plant geographical studies over extensive regions of the globe.

Normalized difference vegetation index (NDVI)

Differences in the spectral reflectance of chlorophyll in the visible and near-infrared parts of the spectrum provide a way to monitor the density and vigor of green vegetation (Tarpley et al. 1984). The National Oceanic and Atmospheric Administration (NOAA) satellite has a five-channel radiometer, the advanced very high resolution radiometer (AVHRR), with channels 1 and 2 in the visible (0.58–0.68 μm) and near-infrared (0.725–1.10 μm) spectral bands respectively. The normalized difference vegetation index (NDVI), which is the best-known vegetation index, is computed using the equation NDVI = (Ch2 – Ch1)/(Ch2 + Ch1), where Ch1 and Ch2 are the

reflectance measurements of AVHRR channels 1 and 2 respectively (Tarpley et al. 1984). The remotely sensed NDVI allows analysis of the "greenness" of vegetation on regional to global scales. The NDVI data, which provide spatially continuous, long-term information on vegetation, are useful for investigating the seasonal vegetation cycle (Gutman 1999).

Many studies have used the remotely sensed NDVI. For example, global vegetation cover has been classified according to the NDVI-derived phenological characteristics of vegetation (Norwine and Greegor 1983; Defries and Townshend 1994). The global land cover characteristics database of Loveland et al. (2000), a detailed global land cover map, used the NDVI to identify land cover. White et al. (1997) developed a continental phenology model of the vegetation of the United States, and compared the result with NDVI data. In addition, attempts have been made to relate the NDVI to meteorological elements, sucn as temperature (Gutman 1991), precipitation (Nicholson et al. 1990; Di et al. 1994; Shinoda 1995), and CO_2 concentration (Tucker et al. 1986).

Background and purpose of the study

This study focused on the phenological characteristics of the vegetation in northern Asia (mainly Siberia) as revealed by the seasonal NDVI cycle, from the perspective of plant geography. Siberia is a key region in climatology and related sciences. A remarkable long-term temperature rise that may be related to global warming has been reported, especially in winter (IPCC 1996, 2001). Ye et al. (1998) addressed long-term changes in snow depth. Myneni et al. (1997, 1998) and Kawabata et al. (2001) pointed out the significant increase in vegetation at high latitudes in the Northern Hemisphere, scrutinizing NDVI data from the 1980s. Tucker et al. (2001) found an increase in the NDVI from 1982 to 1991 and from 1992 to 1999 in higher northern latitudes. Furthermore, the thick taiga forest over the extensive region provides water vapour to the atmosphere via transpiration (Suzuki et al. 1998). Vegetation data should give proxy information on transpiration from the ground, so this study will improve understanding of the water cycle over an extensive area.

As part of the GEWEX Asian Monsoon Experiment (GAME), an international project that is part of the Global Energy and Water Cycle Experiment (GEWEX), GAME-Siberia was implemented in the Lena River basin, and focused on energy and water cycle processes (GAME-International Science Panel 1998). The results of this study are expected to produce meaningful knowledge of hydrometeorological processes over Siberia and in the global climate system. Moreover, the knowledge provided by this study will play an important role in attempts to understand hydrological cycles over Siberia, extending the horizontal scale from the Lena River basin to the entire Siberia region.

Some studies targeting the phenological characteristics of vegetation, as revealed by the seasonal NDVI cycle, have been published. Reed et al. (1994) developed a method to monitor phenological variablility using the seasonal NDVI cycle, and applied it to land cover in the United States. Schwarts (1994) discussed the importance of the NDVI in studying the phenology of the vegetation of North America. However, neither study mentioned phenology in northern Asia. Moulin et al. (1997) visulalized the phenological evolution (dormancy, growth, and senescence) of global vegetation by analyzing the seasonal variation in the NDVI. However, such a global-scale study provides only crude information on localities in northern Asia.

This work was carried as part of two studies: (1) Suzuki et al. (2000), which revealed a close relationship between the NDVI and the geographical distribution of temperature and precipitation along north–south transects in Siberia; and (2) Suzuki et al. (2001a), which examined the phenological regionality of the NDVI and the climate over all of Siberia. The latter study, using monthly NDVI data, reported a west–east difference in the timing of the vegetation cycle in Siberia. The present study established a west–east transect, and compared the west–east vegetation phenology examined using the *weekly* NDVI on an annual basis in Siberia and some surrounding areas. For investigating the phenological features of the vegetation in detail, weekly temporal resolution has a great advantage over the monthly NDVI data used in Suzuki et al. (2001a). The west–east NDVI contrast will be discussed in relation to seasonality in the surface air temperature, precipitation, snow depth, and soil moisture. The result of this study will lead to a better understanding of the essential climatological implications of seasonal vegetation change.

Materials and methods

The region targeted by the analysis is bounded by 30°E and 145°E longitude, and 40°N and 75°N latitude, as indicated in Fig. 1. This region covers Siberia, and parts of European Russia, Mongolia, and China. This study analyzed the weekly NDVI and hydrometeorological measurements made at surface stations, averaged for 1987–1991 (5 years). These years were chosen after considering the availability of temperature, precipitation, and NDVI data. We regard the 5-year mean values for these 5 years as representative of the normal values of those parameters. For some datasets, however, time spans other than 1987–1991 were selected because of the unavailability of data for 1987–1991.

Weekly NDVI data

The second-generation weekly global vegetation index (GVI) data from 1987 to 1991 were used in this study. They were constructed following three sets of procedures (Kidwell 1990; Tarpley 1991):

1. The original AVHRR data with a 1-km resolution obtained on each orbital pass are sampled (every third scan line and then four pixels out of five in that scan line) and averaged, to derive 3 × 5-km resolution data, called the GAC (global area coverage) data.

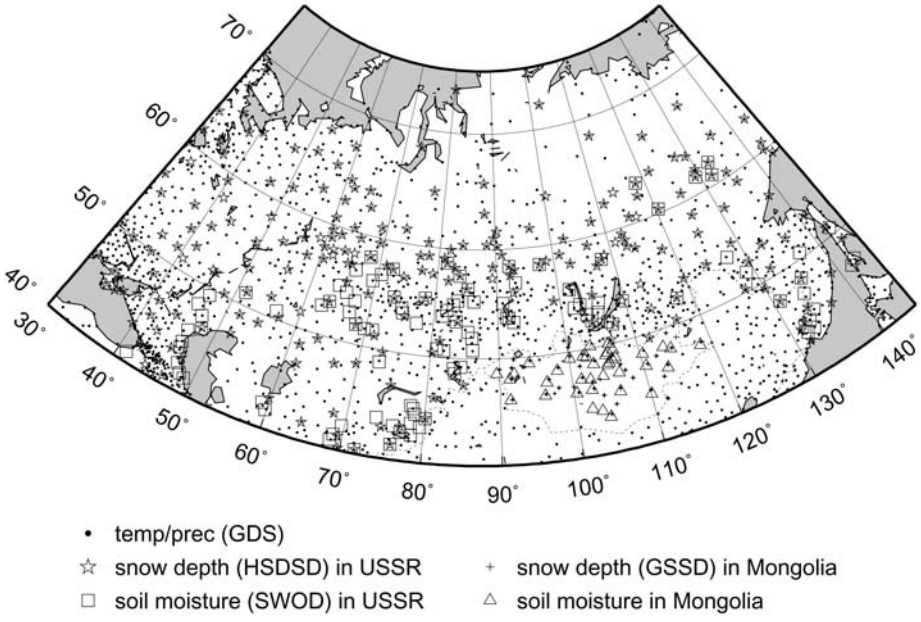

Fig. 1 The study area, the distribution of Global Daily Summary (GDS), Historical Soviet Daily Snow Depth (HSDSD), Federal Climate Complex Global Surface Summary of Day Data Version 6 (GSSD), gravimetric soil moisture covering the USSR (SWOD) stations, and the soil moisture in Mongolia

2. The global daily composite is generated from the GAC for daylight passes of the afternoon polar orbiter. This is called the "daily master array", and has a resolution of 0.144° × 0.144°.
3. From the daily master array, the weekly GVI data, which have the same spatial resolution as the daily master array, are produced. To construct the weekly (7-day) NDVI, only the NDVI for the day with the largest (channel 2 – channel 1) (both digital counts) difference in the AVHRR is retained at each array location for the 7 days (i.e., no averaging process is used). This eliminates clouds from the weekly composite, except for areas that were cloudy on all 7 days.

The weekly GVI still has unrealistic NDVI values, which are probably due to the process of data construction and cloud contamination. For this reason, this study carried out two smoothing processes: smoothing in the horizontal domain, followed by smoothing in the time domain. For horizontal smoothing, (1) the NDVI value at a pixel (NDVI-a) was compared with the mean NDVI (NDVI-m) for the eight pixels adjacent to the NDVI-a pixel; (2) if the difference between NDVI-a and NDVI-m exceeded 0.1, NDVI-a was replaced by NDVI-m; (3) this horizontal smoothing process was executed on all GVI pixels, except for the pixels on the west, east, south, and north boundaries of the study area.

For temporal smoothing, a 3-week moving maximum was calculated. For week n, the highest NDVI value among weeks $n-1$, n, and $n+1$ was adopted as the NDVI value of week n for each pixel. The NDVI values for the first and last weeks in the study period were eliminated from the analysis. Although this process reduces the temporal resolution of the NDVI, it produces a more realistic seasonal cycle of the weekly NDVI.

As summarized by Goward et al. (1993), the GVI data product includes problems that originate in the latitudinal difference in the geometry of the sun, the earth's surface, and the satellite, and in the process of constructing the GVI from the high-resolution dataset. Although the GVI used in this analysis may still contain some unfavorable biases or errors in the data product, we believe that the GVI data are of sufficient accuracy for this study, which discusses the west–east contrast of the NDVI in the same latitudinal zone; the winter NDVI is of no concern. Although the GVI reliability for interannual variation analysis is suspect, as with other global NDVI datasets, the GVI has sufficient reliability for a phenology (seasonal cycle) analysis, as noted by Gutman (1999). The weekly temporal resolution of the GVI data product should be preferable to other, 10-day, global NDVI datasets for analysis of vegetation phenology.

Temperature and precipitation data

Surface air temperature and precipitation data from 1987 to 1991 were obtained from the CD-ROM Global Daily Summary (GDS), which is available from the National Climate Data Center (NCDC) of the NOAA (National Climate Data Center 1994). The GDS contains daily maximum/minimum temperatures, daily precipitation, and 3-h weather data at 10,277 surface WMO stations around the world. There were 1,635 GDS stations in the region analyzed, as shown in Fig. 1.

Snow cover area map

The snow cover information shown in Figs. 2 and 3 was acquired by analyzing data (1987–1991) from the "weekly digital Northern Hemisphere snow and ice product", a satellite-derived snow cover map that is compiled by the NOAA National Environmental Satellite, Data and Information Service (NESDIS). This dataset contains information on the presence or absence of snow cover in each of 89 × 89-square gird boxes on a polar sterographic map that covers most of the Northern Hemisphere (Masuda et al. 1993).

Snow depth data

Snow depth is one of the climatic parameters used to discuss vegetation phenology. Snow depths at surface stations were obtained from the CD-ROM of the Historical Soviet Daily Snow Depth (HSDSD) version 2.0 (Armstrong 2001), which includes daily snow depths at 284 WMO stations, from 1881 (for the earliest operational stations) through 1995. The stations' distribution is shown in Fig. 1.

Snow depths in Mongolia are not covered by the HSDSD, and no suitable dataset was found for the period from 1987 to 1991 that this study examined. As alternative snow depth information for Mongolia, we used snow depths from 1994 to 1996 provided in the Federal Climate Complex Global Surface Summary of Day Data Version 6 (referred to as GSSD in this paper), which was provided by the National Climatic Data Center (National Climatic Data Center 2001). This dataset archives daily surface meteorological properties at over 8,000 WMO stations worldwide. The 51 stations in Mongolia are shown in Fig. 1. Although the difference in periods limits the discussion in terms of snow depth in Mongolia, the data do provide ancillary information.

Soil moisture data

Gravimetric soil moisture data covering the USSR at 115 surface stations (referred to as SWOD) were used. This dataset was constructed mainly from information in the Agrometeorology Yearbook, which is archived by regional meteorological centers in Russia. Observations were made on the 8th, 18th and 28th of each month from April to October. Since data from 1988 to 1991 are not available in SWOD, the SWOD data from 1985 to 1987 were used as alternative information. As with the snow depth data for Mongolia, the different time span limits discussion in terms of soil moisture in the USSR. However, the data do provide ancillary information. The total soil moisture (volumetric) in the 0–10-cm depth layer was used for the analysis.

Soil moisture data for Mongolia are available at 42 stations on the 7th, 17th, and 27th of every month from April to October for the period from 1964 to 1993 (Robock et al. 2000). All the observations were made using the gravimetric technique for each 10-cm layer down to a depth of 1 m, with the first layer divided into two 5-cm layers. The data are volumetric plant-available soil moisture. For our analysis, the original plant-available soil moisture was adjusted according to the wilting level correction table, which was prepared by the dataset producers for each station. This analysis used the plant-available soil moisture in the 5–10 cm depth layer from 1987 to 1991 in Mongolia.

Construction of 5-year mean weekly data

The NDVI data for the leap year (1988) have an extra overlapping week; that is, the 15th week covers 8–14 April, while the 16th week covers 11–18 April, and the 17th week covers 18–24 April. In order to match the weeks with those in other years, the 16th week in 1988 was omitted (to give 52 weeks in each year). Moreover, there are small differences in the calendar dates that the weeks span (i.e., the dates of the beginning and end of each week) in the weekly NDVI and weekly snow cover data, as shown in Table 1.

Table 1 The first date of the first week of the weekly normalized difference vegetation index (NDVI) and snow cover data in each year.

Year	NDVI	Snow cover
1987	1 Jan 1987	29 Dec 1986
1988	1 Jan 1988	4 Jan 1988
1989	2 Jan 1989	2 Jan 1989
1990	1 Jan 1990	1 Jan 1990
1991	31 Dec 1990	31 Dec 1990

The small shift in the dates of the weeks in each year was ignored in the analysis, and it was assumed that the first week in each of the 5 years started on the 1st of January (see Table 2). The 5 year mean of the weekly NDVI was calculated by averaging the weekly NDVIs values for the corresponding weeks from 1987 to 1991. As for the 5-year mean weekly snow cover, a pixel with a snow cover frequency exceeding 50% in a week was regarded as a "snow-cover existing pixel" on a weekly basis.

The first and last weeks of the year were not calculated because of the 3-week moving maximization process that was used for the NDVI time series. The 5-year mean NDVI values and snow cover from the 2nd (8–14 January) to 51st (17–23 December) weeks were derived.

The weekly mean temperature and weekly precipitation for the 5 years were calculated by slotting GDS daily data into NDVI weeks, as shown in Table 2. The daily temperature was calculated using $(T_{d\ max}+T_{d\ min})/2$, where $T_{d\ max}$ and $T_{d\ min}$ are the daily maximum and minimum temperatures, respectively (the daily mean temperature is not available in the GDS).

The daily HSDSD and GSSD snow depth data were also slotted into the weeks (Table 2), and the weekly means calculated. The soil moisture values used were the original three time month^{-1} values, i.e., they were not converted into weekly values.

Results

The NDVI seasonal cycle and its spatial distribution

General features of NDVI distribution

Six examples of the 5-year mean weekly NDVI distribution are shown in Fig. 2. As ancillary information, the 5-year mean weekly snow cover is shown.

In the 9th week (26 February to 4 March), most regions are snow-covered, and the NDVI is very small. The NDVI is slightly higher in the central area (80–110°E, 50–60°N), probably because of the exposed green canopy of non-deciduous forest (Suzuki et al. 2001a). On the basis of information for one site in a taiga forest near Yakutsk, Suzuki et al. 2001b showed that the forest canopy is exposed (no rime or snow accreted) from late winter to spring, when the ground is snow covered.

In spring (30 April–6 May; 18th week), vegetation activity is clearly detected by the NDVI distribution. The

Table 2 The weeks used in the analysis according to calendar date

Week	Date	Week	Date	Week	Date
2	8–14 Jan	18	30 Apr–6 May	35	27 Aug–2 Sep
3	15–21 Jan	19	7–13 May	36	3–9 Sep
4	22–28 Jan	20	14–20 May	37	10–16 Sep
5	29 Jan–4 Feb	21	21–27 May	38	17–23 Sep
6	5–11 Feb	22	28 May–3 Jun	39	24–30 Sep
7	12–18 Feb	23	4–10 Jun	40	1–7 Oct
8	19–25 Feb	24	11–17 Jun	41	8–14 Oct
9	26 Feb–4 Mar	25	18–24 Jun	42	15–21 Oct
10	5–11 Mar	26	25 Jun – 1 Jul	43	22–28 Oct
11	12–18 Mar	27	2 – 8 Jul	44	29 Oct–4 Nov
12	19–25 Mar	28	9–15 Jul	45	5–11 Nov
13	26 Mar – 1 Apr	29	16–22 Jul	46	12–18 Nov
14	2–8 Apr	30	23–29 Jul	47	19–25 Nov
15	9–15 Apr	31	30 Jul – 5 Aug	48	26 Nov–2 Dec
16	16–22 Apr	32	6–12 Aug	49	3–9 Dec
17	23–29 Apr	33	13–19 Aug	50	10–16 Dec
		34	20–26 Aug	51	17–23 Dec

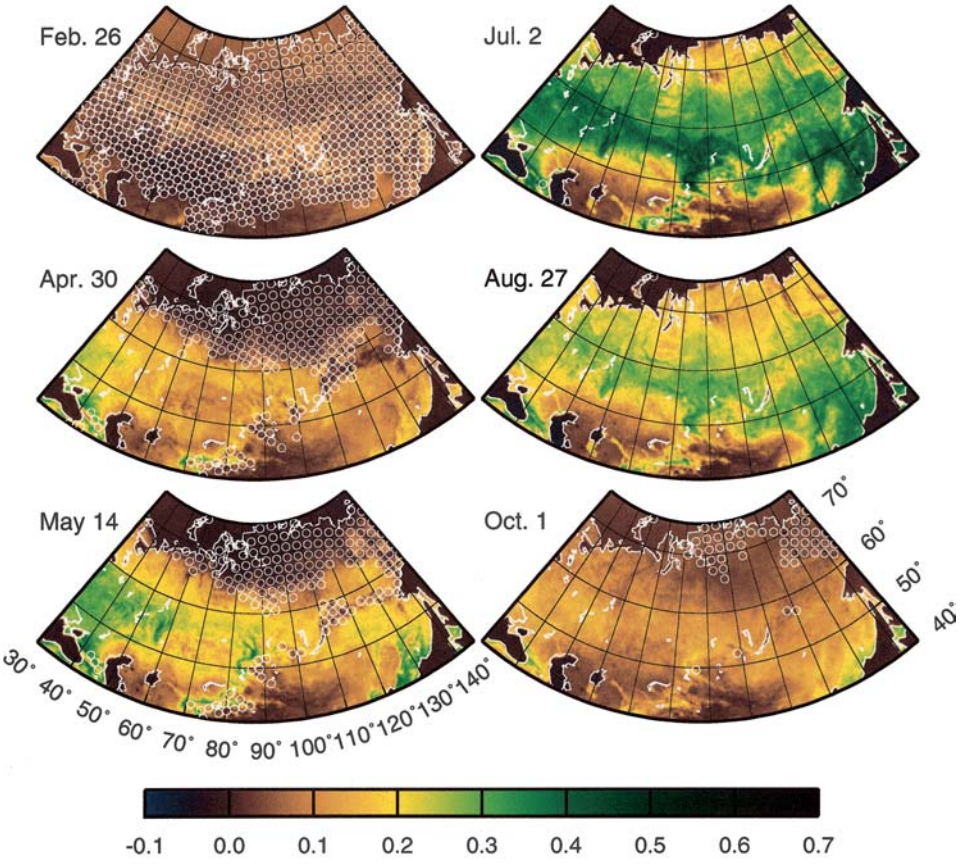

Fig. 2 Six examples of the weekly normalized difference vegetation index (NDVI) distribution. The date to the left of each map is the first date of the respective week. ◯ Snow cover

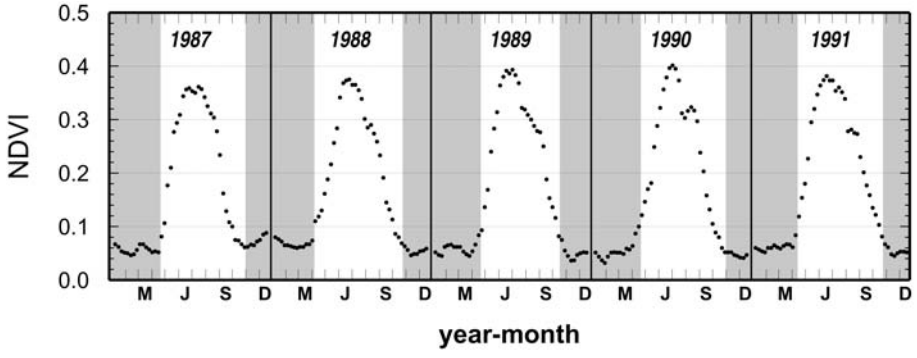

Fig. 3 Weekly change in the NDVI averaged in the region bounded by 50°E, 90°E, 55°N, and 60°N. *Hatched area* The period of snow cover calculated from the National Oceanic and Atmospheric Administration (NOAA) / National Environmental Satellite Data and Information Service (NESDIS) snow cover data

first area showing green-up of the NDVI is located in the western part of the region (30–40°E, 40–60°N). Moreover, with the northward recession of the snow cover, the NDVI increases slightly in the snow-cleared area. In mid May (14–20 May; 20th week), the green-up extends eastward, and forms a west–east green zone, while the NDVI also starts to increase in the southeastern area (around 130°E, 45°N). This green-up is attributed to foliation of the forest ecosystem.

In July, the foliage in most of Siberia is mature. The snow cover has melted completely, and an extensive high-NDVI (over 0.4) zone is seen between 50°N and 60°N latitude (2–8 July; 27th week). This high-NDVI zone roughly corresponds to the forest area (Suzuki et al. 2000). In the area south of 50°N, except east of 115°E, the NDVI is small, due to arid land cover types, such as the Kazakh steppe, Kyzylkum desert, Takla Makan desert, and Gobi desert. The NDVI over the tundra vegetation in the Arctic is also relatively small.

August is generally the beginning of the senescence season for vegetation in Siberia. In the week from 27 August to 2 September (35th week), an extensive green

area can be seen between 50° and 60°N, but the NDVI is lower than in July. The NDVI in the southeastern area is still large, while the NDVI in the western area is significantly lower than in July. In autumn, the vegetation changes from the senescence to the dormancy phase. The NDVI is small, as in winter, and snow cover is seen in the northern part of the region (1–7 October; 40th week).

Spatial features of phenological events

The results in the previous section tell us that the phenological characteristics differ with area. In this section, 3 specific weeks are picked as parameters reflecting the phenological events of the vegetation: (1) green-up, defined as the week when the NDVI first exceeds 0.2 in the year (W-a), (2) maximum, defined as the week when the annual maximum NDVI occurs (W-b), and (3) senescence, defined as the first week after the maximum that the NDVI drops below 0.2 (W-c).

An NDVI threshold of 0.2 was selected for W-a and W-c. This value is slightly higher than in previous research; Malingreau (1986), for example, defined the growing season as the period with an NDVI higher than 0.1, while Lloyd (1990) regarded the growing season as the period when the NDVI exceeded 0.099. We chose a rather higher threshold because we had to consider the effect of snow, which covers most of the region from autumn to spring, in the seasonal NDVI cycle.

Figure 3 shows the snow-covered period and the weekly NDVI averaged for the region 50–90°E, 55–60°N, as an example. This figure demonstrates that the NDVI increases abruptly and exceeds 0.1 as the snow melts. Since the NDVI of a snow-covered surface is smaller than that of other land surfaces because of its spectral characteristic, this abrupt increase might include a component that is due to the thaw itself. Therefore, to examine changes in vegetation, we set the NDVI threshold at 0.2.

The distribution of these three specific parameters is examined in Fig. 4. GVI pixels in which the NDVI did not exceed 0.2 years-round were excluded from this analysis (indicated in gray in Fig. 4).

The area with the earliest W-a, before the 18th week (30 April–6 May), was located mainly around the Black and Caspian Seas. W-a was relatively early (18th–22nd week) in a zone (west–east) roughly between 50° and 60°N (referred to as the 50-60°N zone). The W-a north of 60°N gradually became later farther northward, and the W-a in tundra areas was after the 29th week (16–22 July). The W-a south of 50°N was also late, especially in the arid area of Mongolia. Within the 50–60°N zone, the W-a gradually became later eastward around Lake Baikal (22nd week; 28 May–3 June) from the western area, while W-a was early (19th week; 7–13 May) near the Sea of Japan coast.

W-b contains more essential information on the vegetation phenology in Siberia than W-a or W-c, because W-a and W-c can change with the definition of the thresshold value (i.e., 0.2) in the seasonal NDVI cycle, while the maximum NDVI is not altered by the definition.

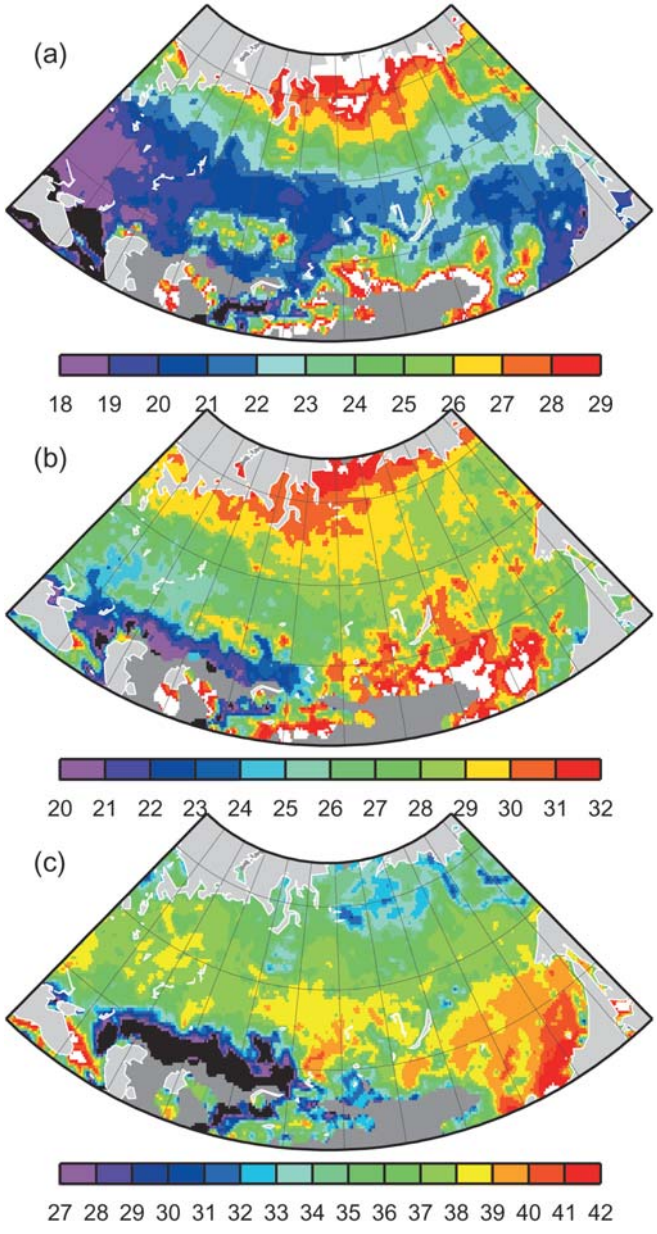

Fig. 4a–c The distribution of the weeks when the NDVI exceeded 0.2 (W-a) (**a**), NDVI reached the annual maximum (W-b) (**b**), and dropped below 0.2 (W-c) (**c**). *Gray* Pixels in which the NDVI did not exceed 0.2, excluded from the analysis. *Black* A pixel with an earlier week than the earliest week on the color scale. *White* A pixel with a later week than the latest week on the color scale

The overall distribution of W-b was similar to that of W-a. W-b occurred earliest in the western region (30–80°E) between 45° and 50°N, which includes the Kazakh steppe, in the 20th week (14–20 May). In contrast, the W-b near the Mongolian steppe was the latest, after the 31st week (30 July–5 August). There was a marked west-early/east-late constrast in the W-b in Kazakh and Mongolia (11 weeks) in the 45–50°N zone. In the 50–60°N zone, there was also a west–east gradient; that is,

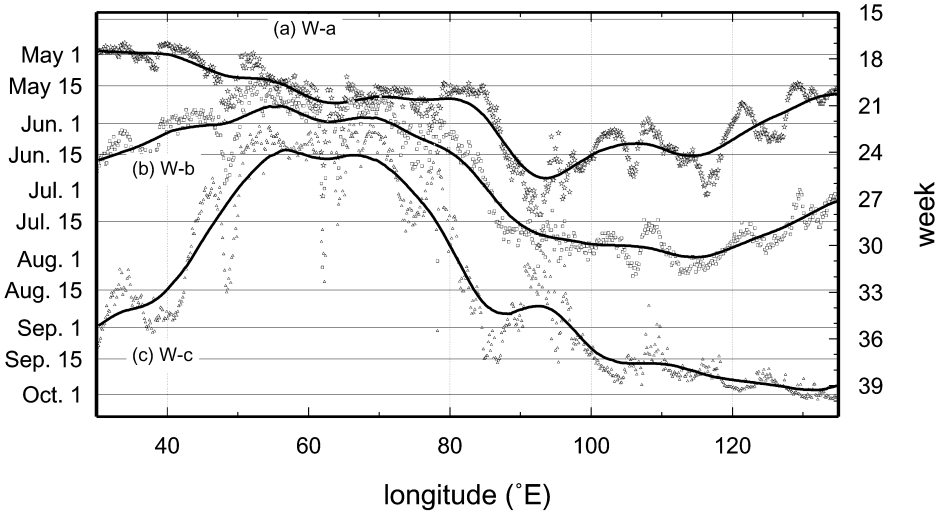

Fig. 5 The west–east profile of the weeks in the 45–50°N zone when the NDVI exceeded 0.2 (*a*), the NDVI annual maximum occured (*b*), and the NDVI dropped below 0.2 (*c*). *Solid line* The smoothed line produced using a low-pass filter

the western area generally had an earlier W-b than the eastern area (especially around Lake Baikal). To the north of the 50–60°N zone, the week gradually became later, and the latest week in the tundra area was the 31st week (30 July–5 August), which was 7 weeks later than in the earliest area.

In the map of W-c, areas with extremely early values (before the 27th week, 2–8 July) are seen in the Kazakh steppe area, similar to the map of W-b, while W-c in the southeast area, including Mongolia, occurred after the 39th week (24–30 September). In the 50–60°N zone, the gradient of W-c is less apparent than those of W-a and W-b.

Using the NDVI, the regional phenology of green-up, maximum, and senescence can clearly be seen using W-a, W-b, and W-c respectively. This study discusses the west–east contrast in the phenological characteristics of W-a, W-b, and W-c in the 45–60°N zone. Although a south-north phenological contrast was also apparent, this west-to-east phenology of NDVI, the so-called gree-wave, is more interesting.

Discussion

This section considers the west–east phenological contrast that is manifested as the green-wave. Two zonal transects, 45–50°N and 50–60°N, were selected to discuss the west–east contrast, and W-a, W-b, and W-c were examined in relation to climatological parameters. The 45–50°N zone corresponds primarily to semi-arid regions that are covered by steppe vegetation, such as the Kazakh and Mongolian steppe. As Suzuki et al. (2000) discussed, the vegetation near Kazakh is strongly dominated by the available water. The 50–60°N zone corresponds to forested regions, including taiga, and a high NDVI west–east zone forms in this transect in summer, as Suzuki et al. (2001a) demonstrated.

West–east phenological contrast in semi-arid area (45–50°N)

As Fig. 4 shows, W-a, W-b, and W-c occur very early near the Kazakh steppe, and form a remarkable west-early/east-late phenological contrast between the Kazakh and Mongolia steppes, which are located at the same latitude. This section focuses on this west–east contrast in the 45–50°N zone and its relation to climatological factors.

Figure 5 shows the mean W-a, W-b, and W-c, averaged over the pixels in individual south-north strips, which were 0.144° longitude wide, in the zone between 45° and 50°N. There were 800 strips from 30°E to 145°E, and each strip contained 34 NDVI pixels. Pixels for which the annual maximum did not exceed 0.2 were excluded from the calculation of the mean values shown in Fig. 5. The smoothed lines were drawn using a low-pass filter that applied a moving-average method with normal curve weights (Holloway 1958). The frequency response of the filter was set to 0.5 at 1 cycle/degree.

For W-a and W-b, a west-early/ease-late gradient was apparent. Near 60°E, W-a and W-b were weeks 20.4 and 21.7, respectively, while near 110°E, they were weeks 23.8 and 30.4. There were 3.4- and 8.7-week time lags in W-a and W-b respectively. W-c was relatively late west of 50°E, whereas it was earliest between 55° and 70°E (i.e., near the Kazakh steppe). W-c was 13.4 weeks earlier near 60°E than near 110°E. Moreover, the time between W-a to W-c was noticeably short (3.8 weeks) in the Kazakh region, illustrating the short growing period there.

As representative of the western and eastern areas in the 45–50°N transect, the Kazakh (45–75°E, 45–50°N) and Mongolia (100–120°E, 45–50°N) areas were selected, and Fig. 6 compares seasonal cycles in weekly temperature, precipitation, snow depth, and soil moisture for the two areas. The soil moisture in the Kazakh area is the mean from 1985 to 1987. The snow depth in the Mongolian area is the mean from 1994 to 1996. The

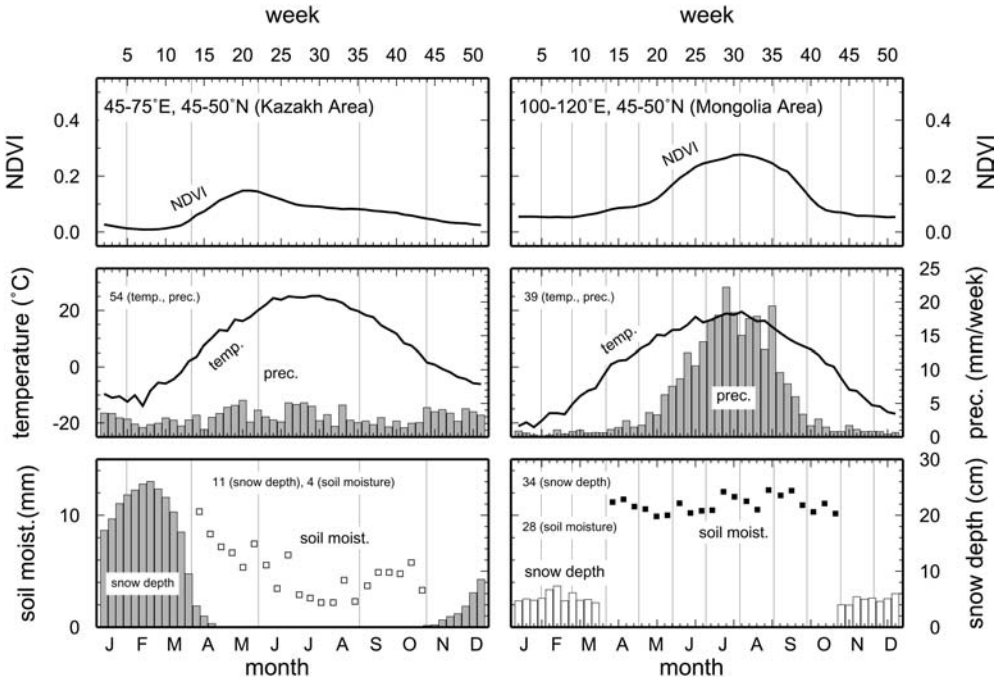

Fig. 6 The seasonal change in the weekly NDVI, temperature, precipitation, snow depth, and 10-day soil moisture in two arid regions: Kazakh (*left*) and Mongolia (*right*) in the 45–50°N zone. The soil moisture for the Kazakh area and the snow depth for the Mongolian area for 1985–1987 and 1994–1996 respectively. Other statistics are the means from 1987 to 1991. The figures in the panel are the number of stations used to calculate the mean temperature, precipitation, snow depth, and soil moisture

other statistics are the means from 1987 to 1991, the actual time span of this study.

As Fig. 6 shows, the seasonal change in the NDVI in the Kazakh area showed early green-up and a short growing period, while that in the Mongolian area exhibited late green-up and a late maximum. Suzuki et al. (2001a) classified seasonal NDVI cycles at 611 sites in Siberia, on the basis of monthly NDVI values, and obtained ten classes for the seasonal NDVI cycle. According to that classification, the Kazakh area is mainly class B, which is characterized by early green-up and low NDVI, while the primary class in the Mongolian area is class D2, which is characterized by a high NDVI and a late maximum. These features are consistent with our results.

Conspicuous differences between these two areas are also seen in their precipitation, snow depth, and soil moisture. In the Kazakh area, the snow was deep (about 26 cm) in late February, and it disappeared in late April. Although soil moisture data before March were unavailable, and the statistical period was from 1985 to 1987, the soil moisture in the Kazakh area was highest (10.3 mm in the surface 10-cm layer) in early April, when the snow had almost finished melting. Subsequently, the soil moisture decreased to a minimum in August. The small amount of precipitation in the Kazakh area (Fig. 6) was insufficient to stop the decrease in soil moisture.

In the Mongolian area, the precipitation showed an obvious unimodal seasonal cycle, with a maximum (22 mm week^{-1}) in mid July. Although the snow was not as deep in winter as in the Kazakh area, the soil moisture remained relatively high (arround 10 mm in the 5–10-cm layer) from April to October.

Figure 7 shows the temporal pattern of NDVI with longitude and precipition in the 45–50°N zone. There is good agreement between the NDVI and precipitation, i.e., areas with high precipitation generally correspond to the high NDVI domain. Especially in the region east of 100°E, there is similar temporal variation in NDVI and precipitation. Green-up of the NDVI coincided with the start of the rainy season in May–June. The maximum NDVI (W-b) occurred at almost the same time as the precipitation maximum. The NDVI decreased with precipitation in the autumn. In other regions with relatively large amounts of precipitation, such as the regions within 30–45°E and 80–87°E, NDVI varied with the seasonal variation in precipitation.

By contrast, between 50° and 80°E, the NDVI was not as high as it was east of 100°E. Instead, a small NDVI maximum was found in early summer, which was seen in the NDVI variation in the Kazakh area (Fig. 6). Although the precipitation in this region was small all year round, deep snow cover prevailed until March. These facts suggest that water is available for vegetation in the Kazakh area only for a very short period after snowmelt, and this season is the only time that vegetation flourishes. Consequently, the vegetation matures in late May when water from melting snow is still abundant in the soil. In addition, the span from W-a to W-c in the Kazakh area is considerably shorter than that in the Mongolian area. In the Mongolian area, large amounts of precipitation in summer support the occurrence of the mature stage of vegetation in midsummer, 8.7 weeks after it occurs in the Kazakh area. It is also possible that the winter soil temperature in the Kazakh area is kept higher by the thick snow cover compared with the Mongolian area, possibly inducing the earlier green-up in the Kazakh area.

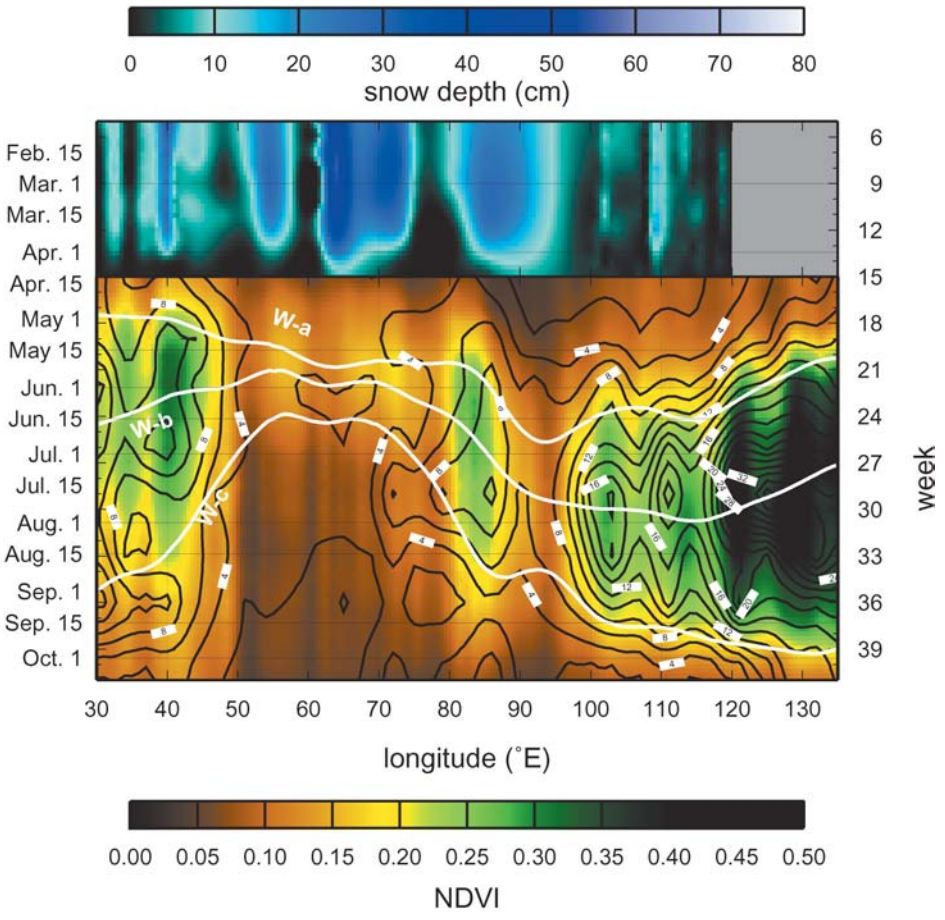

Fig. 7 Time longitude cross-section of the NDVI (*color scale*) and precipitation (*black contour*: mm week^{-1}) from the 15th to 40th weeks, and the snow depth (cm) from the 5th to 14th weeks in the 45–50°N zone. The snow depth east of 120°E was not plotted owing to an insufficient number of stations. W-a, W-b, and W-c are superimposed

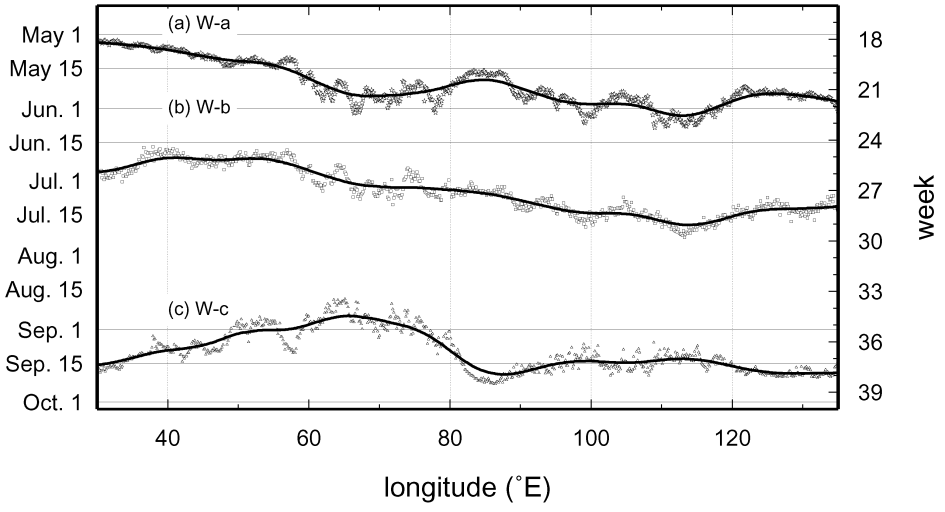

Fig. 8 The west–east profile of the week in the 50–60°N zone when the NDVI exceeded 0.2 (*a*), the NDVI annual maximum occured (*b*), and the NDVI dropped below 0.2 (*c*). *Solid line* The smoothed line produced using a low-pass filter

West–east phenological contrast in forest area (50–60°N)

Figure 8 shows the mean W-a, W-b, and W-c in the zone between 50° and 60°N. There were 800 strips from 30°E to 145°E, and each strip had 69 pixels. The smoothed line was drawn as in Fig. 5. Likewise, pixels for which the annual maximum did not exceed 0.2 were excluded for the calculations of mean value.

The west-early/east-late gradient of the W-a and W-b zonal profiles is obvious in these graphs. Around 40°E, W-a occurred at about 18.6 weeks (beginning of May), while W-a near 115°E was at 22.4 weeks (beginning of June), i.e., green-up at 40°E was 3.8 weeks earlier than that at 115°E. W-b shows a similar profile. W-b near 40°E was at about 25.1 weeks (mid June), while W-b near

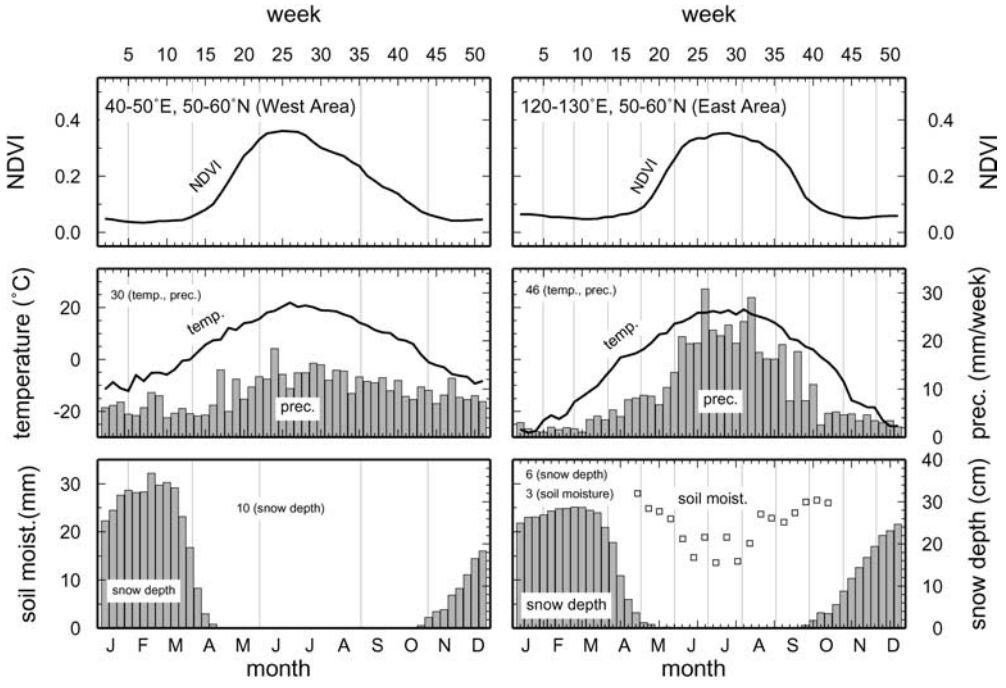

Fig. 9 The seasonal change in the weekly NDVI, temperature, precipitation, snow depth, and 10-day soil moisture in two forest areas: the west (*left*) and east (*right*) areas in the 50–60°N zone. The soil moisture data in the east area is from 1985 to 1987; soil moisture for the west area was not available. The other statistics are the means from 1987 to 1991. The figures in the panel are the number of stations used to calculate the mean of temperature, precipitation, snow depth, and soil moisture

115°E was at about 29.0 weeks (mid July), a 3.9-week difference.

W-a and W-b east of 115°E were progressively earlier. However, the west-early/east-late pattern for W-a and W-b is a general characteristic of the zonal profile in the Siberian vegetation phenology. No zonal trend is apparent for W-c. The earliest W-c (34.4 weeks, end of August) was at 65.6°E, and the latest W-c (37.9 weeks, mid September) was near 87.6°E.

As for the analysis for the 45–50°N zone, the seasonal cycles of the weekly temperature, precipitation, snow depth, and 10-day soil moisture in the west (40–50°E, 50–60°N) and east (120–130°E, 50–60°N) areas are compared in Fig. 9. Unfortunately, no soil moisture data are available for the west area because there is no SWOD station in this area. The soil moisture plot for the east area is the mean from 1985 to 1987. The west area is predominantly class E2 according to the classification by Suzuki et al. (2001a), while the primary classes in the east area are D1 and F. These three classes have large amplitudes in the seasonal NDVI cycle, and class E2 is characterized by early occurrence of the maximum NDVI. These features agree well with the results of this study, as indicated in Fig. 9.

In Fig. 9, there is an obvious difference in the timing of the phenology between the west and east areas in the 50–65°N zone. W-a in the west area occured around the beginning of March, while it occurred around mid May in the east area. W-b occurred in the 25th week (18–24 June) in the west area and in the 29th week (16–22 July) in the east area, i.e., it was 4 weeks earlier in the west.

Although no obvious difference like that found in the 45–50°N zone is seen, there are some differences in the seasonal temperature cycle in the 50–60°N transect. The annual range of temperature in the east area (about 48 °C) is much greater than in the west area (34 °C). This is mainly due to the much colder winters in the east area (–28.3 °C in the 3rd week) than in the west (–12.1 °C in the 5th week).

To discuss the relationship between temperature and vegetation, a cumulative measure of temperature from the beginning of the year is often used, such as the warmth index (Kira 1948) or modified warmth index (Suzuki et al. 2000). This analysis examined the cumulative weekly mean temperature exceeding 0 °C at each staton from the beginning of the year (T_c), based on the threshold temperatures established in Suzuki et al. (2000) for Siberian vegetation.

Figure 10 shows the weeks in which T_c exceeded 40 °C (W-40) and 140 °C (W-140). This plot reveals a west-early/east-late trend in the profiles of both W-40 and W-140. Near 40°E, W-40 and W-140 occur in roughly the 19th (early May) and 25th (late June) weeks, respectively. Near 112°E, the respective times are the 23rd (early June) and 30th (late July) weeks. East of 112°E, there is a slight increase in both W-40 and W-140. This west–east trend is quite similar to the trends in W-a and W-b shown in Fig. 8. Figure 11 contains scatter diagrams of W-a/W-40 and W-b/W-140. There are linear relationships with high correlation coefficients for both plots (0.81 for W-a and W-40, 0.84 for W-b and W-140).

These results suggest that the west-fast/east-slow temperature accumulation in the seasonal cycle plays an important role in the climatological environment that characterizes the west-early/east-late times of the green-up and the mature state of vegetation. In this analysis, the critical values of the cumulative temperature (i.e., 40 °C and 140 °C) were determined by trial and error. In

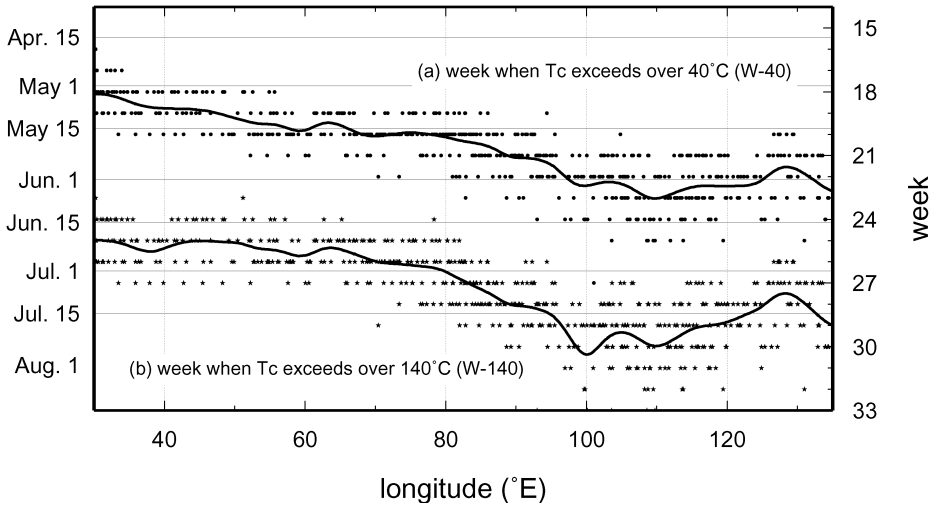

Fig. 10 The west–east profile of the week in the 50–60°N zone when T_c exceeded 40 °C (*a*; *dots*) and T_c exceeded 140 °C (*b*; *stars*)

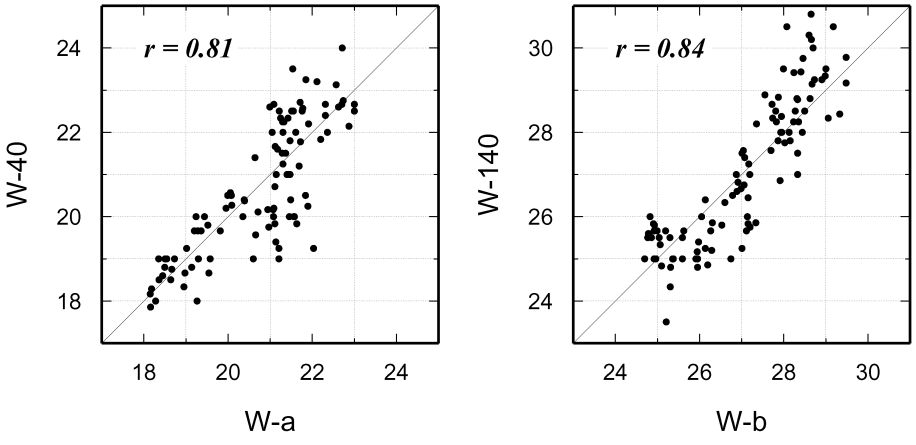

Fig. 11 Correlations between W-a and W-40 (*left*) and W-b and W-140 (*right*)

addition, the result of the W-a/W-40 relation depends on the definition of the threshold NDVI for W-a, i.e., 0.2 in this study. Although it is not clear why cumulative temperatures of 40 °C and 140 °C specifically correspond to W-a and W-b respectively, the climatological environment may have implications for plant physiology. These critical values may change with climatic and vegetation zone, and such an analysis will be performed on a global scale in the future.

Conclusions

The phenological regionality of the vegetation in north Asia was investigated using remotely sensed NDVI data. The 5-year (1987–1991) mean weekly NDVI time series was calculated from the second-generation weekly GVI dataset, which covers the earth with a 0.144° spatial resolution. Temperature, precipitation, snow depth, and soil moisture seasonal cycles were examined to interpret the seasonal NDVI cycle.

In winter, the NDVI is very low throughout the region. Beginning at the end of April, green-up occurs in the western part of the region, and a high NDVI west–east zone forms at 50–60°N latitude in summer. The NDVI in the southern arid area and northern tundra is never high, even in summer. In the autumn, the NDVI drops, and the dormancy season occurs in winter, when the NDVI is once again small throughout the region.

An NDVI green-wave propagating from west to east was seen in the 45–60°N zone in the analysis of weekly data that reflects a phenological time lag between the western and eastern parts of the study area. Three phenological events were defined and calculated for each pixel: green-up (W-a), maximum (W-b), and senescence (W-c) weeks. Generally, there was a west-early/east-late spatial gradient in all three events. In the zone between 45° and 50°N, green-up, maximum, and senescence occurred near 60°E (Kazakh) about 3.4, 8.7, and 13.4 weeks earlier than near 110°E (Mongolia) respectively. The vegetation in Kazakh flourishes during a short period when snowmelt is available from late spring to early summer, while in Mongolia, abundant water is available for the vegetation, even in midsummer, because of the large amount of precipitation.

In the 50–60°N zone, W-a and W-b near 40°E were respectively about 3.8 and 3.9 weeks earlier than they were near 115°E. There was no clear west–east gradient

in W-c. This west-early/east-late phenological contrast was related to the weekly cumulative temperature (over 0 °C). The weeks in which the cumulative temperature exceeded 40 °C and 140 °C had a west–east trend very similar to those of the green-up and maximum weeks of the NDVI, respectively.

Remotely sensed NDVI data revealed aspects of the phenology of the vegetation in north Asia. The essential relationship between the vegetation and climate in Siberia was dominated by moisture in the 45–50°N zone and by temperature in the 50–60°N zone. These results agree quite well with the results of Suzuki et al. (2000), who investigated their relationship in south-north transects.

This paper has highlighted west–east differences in the seasonal cycle and discussed their climatological background. These results improve our knowledge of the climate and of the phenology and distribution of vegetation. Moreover, the results improve our understanding of the impact of vegetation on climate over an extensive area of the globe. In the future, these results will be compared to surveys of other terrestrial areas to evaluate other vegetation-climate relationships. Topography, soil type, and permafrost can also influence vegetation. These relationships could be the target of a future study using the NDVI.

Acknowledgements The authors thank Dr. Dennis Dye (Frontier Research System for Global Change) for his suggestions and advice, and the referees for their useful comments, which contributed to the final version of the manuscript. All the pictures were constructed with the help of the GMT System (Wessel and Smith 1991). This study was partly supported by a grant-in-aid of scientific research from the Ministry of Education, Science, Sports, and Culture, Japan ("Better Understanding of Water and Energy Circulation on a Continental Scale based on Satellite Remote Sensing"; 08241105).

References

Armstrong R (2001) Historical Soviet daily snow depth. Version 2 (HSDSD). National Snow and Ice Data Center, Boulder Colo. CD-ROM

Defries RS, Townshend JRG (1994) NDVI-derived land cover classifications at a global scale. Int J Remote Sens. 15:3567–3586

Di L-P, Lundquist DC, Han L-H (1994) Modelling relationships between NDVI and precipitation during vegetative growth cycles. Int J Remote Sens. 15:2121–2136

GAME-International Science Panel (1998) GEWEX Asian monsoon experiment (GAME) implementation plan. GAME-International Science Panel, GAME International Project Office, Hydrospheric Atmospheric Research Center, Nagoya University

Goward SN, Dye DG, Turner S, Yang J (1993) Objective assessment of the NOAA global vegetation index data product. Int J Remote Sens. 14:3365–3394

Gutman GG (1991) Monitoring land ecosystems using the NOAA global vegetation index dataset. Palaeogeogr Palaeoclimatol Palaeoecol (Global Planet Change Sect) 90:195–200

Gutman G (1999) On the use of long-term global data of land reflectance and vegetation indices derived from the advanced very high resolution radiometer. J Geophys Res 104:6241–6255

Holloway JL Jr (1958) Smoothing and filtering of time series and space fields. Adv Geophys 4:351–389

IPCC (1996) Climate change 1995: the science of climate change. In: Houghton JT, Meira Filho LG, Callander BA, Harris N, Kattenberg A, Maskell K (eds) Contribution of working group I to the second assessment report of the Intergovernmental Panel on Climate Change. Cambridge University Press, Cambridge

IPCC (2001) Climate change 2001: the scientific basis. In: Houghton JT, Ding Y, Griggs DJ, Noguer M, Linden PJ van der, Dai X, Maskell K, Johnson CA (eds) Contribution of working group I to the third assessment report of the Intergovernmental Panel on Climate Change. Cambridge University Press, Cambridge

Kawabata A, Ichii K, Yamaguchi Y (2001) Global monitoring of interannual changes in vegetation activities using NDVI and its relationships to temperature and precipitation. Int J Remote Sens. 22:1377–1382

Kidwell KB (1990) Global vegetation index user's guide. U.S. Department of Commerce, NOAA, NESDIS, NCDC, SDSD

Kira T (1948) On the altitudinal arrangement of climatic zones in Japan. A contribution to the rational land utilization in cool highlands. Agric Sci North Temperate Region 2:143–173 (in Japanese)

Lloyd D (1990) A phenological classification of terrestrial vegetation cover using shortwave vegetation index imagery. Int J Remote Sens. 11:2269–2279

Loveland TR, Reed BC, Brown JF, Ohlen DO, Zhu J, Yang L, Merchant JW (2000) Development of a global land cover characteristics database and IGBP DISCover from 1-km AVHRR Data. Int J Remote Sens. 21:1303–1330

Malingreau J-P (1986) Global vegetation dynamics: satellite observations over Asia. Int J Remote Sens 7:1121–1146

Masuda K, Morinaga Y, Numaguti A, Abe-Ouchi A (1993) The annual cycle of snow cover extent over the Northern Hemisphere as revealed by NOAA/NESDIS satellite data. Geogr Rep Tokyo Metropolitan University 28:113–132

Moulin S, Kergoat L, Viovy N, Dedieu G (1997) Global-scale assessment of vegetation phenology using NOAA/AVHRR satellite measurements. J Clim 10:1154–1170

Myneni RB, Keeling CD, Tucker CJ, Asrar G, Nemani RR (1997) Increased plant growth in the northern high latitudes from 1981 to 1991. Nature 386:698–701

Myneni RB, Tucker CJ, Asrar G, Keeling CD (1998) Interannual variations in satellite-sensed vegetation index data from 1981 to 1991. J Geophys Res 103:6145–6160

National Climatic Data Center (1994) Global daily summary (CD-ROM)

National Climatic Data Center (2001) Federal climate complex global surface summary of data version 6 (ftp://ftp.ncdc.noaa.gov/)

Nicholson SE, Davenport ML, Malo AR (1990) A comparison of the vegetation response to rainfall in the Sahel and East Africa, using normalized difference vegetation index from NOAA AVHRR. Clim Change 17:209–241

Norwine J, Greegor DH (1983) Vegetation classification based on advanced very high resolution radiometer (AVHRR) satellite imagery. Remote Sens Environ 13:69–87

Reed BC, Brown JF, VanderZee D, Loveland TR, Merchant JW, Ohlen DO (1994) Measuring phenological variability from satellite imagery. J Veg Sci 5:703–714

Robock A, Vinnikov KY, Srinivasan G, Entin JK, Hollinger SE, Speranskaya NA, Liu S, Namkhai A (2000) The global soil moisture data bank. Bull Am Meteorol Soc 81:1281–1299

Schwarts MD (1994) Monitoring global change with phenology: the case of the spring green wave. Int Biometeorol 38:18–22

Shinoda M (1995) Seasonal phase lag between rainfall and vegetation activity in tropical Africa as revealed by NOAA satellite data. Int J Climatol 15:639–656

Suzuki R, Yatagai A, Yasunari T (1998) Satellite-derived vegetation index and evapotranspiration estimated by using assimilated atmospheric data over Asia. J Meteorol Soc Jpn 76:663–671

Suzuki R, Tanaka S, Yasunari T (2000) Relationships between meridional profiles of satellite-derived vegetation index (NDVI) and climate over Siberia. Int J Climatol 20:955–967

Suzuki R, Nomaki T, Yasunari T (2001a) Spatial distribution and its seasonality of satellite-derived vegetation index (NDVI) and climate in Siberia. Int J Climatol 21:1321-1335

Suzuki R, Yoshikawa K, Maximov TC (2001b) phenological photographs of Siberian larch forest from 1997 to 2000 at Spasskaya Pad, Republic of Sakha, Russia. http://picard.suiri.tsukuba.ac.jp/~siberia/spaphoto/index/index.htm

Tarpley JD (1991) The NOAA global vegetation index product – a review. Palaeogeorgr Palaeoclimatol Palaeoecol (Global Planet Change Sect) 90:189–194

Tarpley JD, Schneider SR, Money RL (1984) Global vegetation indices from the NOAA-7 meteorological satellite. J Clim Appl Meteorol 23:491–494

Tucker CJ, Fung IY, Keeling CD, Gammon RH (1986) Relationship between atmospheric CO_2 variations and a satellite-derived vegetation index. Nature 319:195–199

Tucker CJ, Slayback DA, Pinzon JE, Los SO, Myneni RB, Taylor MG (2001) Higher northern latitude normalized difference vegetation index and growing season trends from 1982 to 1999. Int J Biometeorol 45:184–190

Walter H (1973) Vegetation of the earth in relation to climate and the eco-physiological condition (translated by Wieser J.) Springer, New York, Berlin Heidelberg

Wessel P, Smith WHF (1991) Free software helps map and display data. EOS Trans AGU 72:441, 445–446

White MA, Thornton PE, Running SW (1997) A continental phenology model for monitoring vegetation responses to interannual climatic variability. Global Biogeochemical Cycles 11:217–234

Woodward FI (1987) Climate and plant distribution. Cambridge University Press, Cambridge

Ye H, Cho H-R, Gustafson PE (1998) The change in Russian winter snow accumulation during 1936–83 and its spatial patterns. J Clim 11:856–863